

1 **Measurement Report: Urban Ammonia and Amines in Houston, Texas**

2
3 Lee Tiszenkel¹, James Flynn², Shan-Hu Lee^{1*}

4
5 ¹ Department of Atmospheric and Earth Sciences, University of Alabama at Huntsville;
6 Huntsville, Alabama, USA

7 ² Department of Earth and Atmospheric Sciences, University of Houston; Houston, Texas,
8 USA

9
10 Corresponding author (shanhu.lee@uah.edu)

11

12 **Abstract.** Ammonia and amines play critical roles in secondary aerosol formation, especially in
13 urban environments. However, fast measurements of ammonia and amines in the atmosphere are
14 very scarce. We measured ammonia and amines with a chemical ionization mass spectrometer
15 (CIMS) at the urban center in Houston, Texas, the fourth most populated urban site in the United
16 States, during October 2022. Ammonia concentrations were on average 4 parts per billion in
17 volume (ppbv), while the concentration of an individual amine ranged from several parts per
18 trillion in volume (pptv) to hundreds of pptv. These reduced nitrogen compounds were more
19 abundant during the weekdays than on weekends and correlated with measured CO concentrations,
20 implying they were mostly emitted from pollutant sources. Both ammonia and amines showed a
21 distinct diurnal cycle, with higher concentrations in the warmer afternoon, indicating dominant
22 gas-to-particle conversion processes taking place with the changing ambient temperatures. Studies
23 have shown that dimethylamine is critical for new particle formation (NPF) in the polluted
24 boundary layer, but currently, there are no amine emission inventories in global climate models
25 (as opposed to ammonia). Our observations made in very polluted Houston, as well as a less
26 polluted site (Kent, Ohio) from our previous study (You et al., 2014), indicate there is a consistent
27 ratio of dimethylamine over ammonia at these two sites. Thus, our observations can provide a
28 relatively constrained proxy of dimethylamine using 0.1% ammonia concentrations at polluted
29 sites in the United States to model NPF processes.

30 **1. Introduction**

31 Atmospheric ammonia and amines are ubiquitous in the atmosphere, and they have been found
32 in the gas phase, aerosol, clouds, and fog droplets (Ge et al., 2011a, b). Ammonia and amines are
33 emitted from various natural and anthropogenic sources, such as agricultural activity, animal
34 husbandry, vegetation, soil, waste processing, automobile traffic, power plants, and biomass
35 burning (Ge et al., 2011a). Ammonia and amines often share the same emission sources. In general,
36 ambient concentrations of ammonia are at the parts per billion in volume (ppbv) range, and amines
37 are approximately two to three orders of magnitude lower than ammonia concentrations. Ambient
38 concentrations of ammonia and amines vary rapidly due to emission, gas-to-particle conversion,
39 and wet deposition processes (You et al., 2014; Yu and Lee, 2012).

40 Laboratory studies have shown that ammonia and amines play key roles in new particle
41 formation (NPF) as they can stabilize sulfuric acid clusters (Yu et al., 2012; Almeida et al., 2013;
42 Lehtipalo et al., 2018; Xiao et al., 2021; Glasoe et al., 2015; Jen et al., 2016). In particular,
43 dimethylamine can have a profound effect on atmospheric processes even at the pptv level
44 (Almeida et al., 2013; Glasoe et al., 2015). Field observations show that ammonia and amines are
45 associated with NPF events in Chinese megacities (Yao et al., 2016; Yan et al., 2021; Cai et al.,
46 2021; Cai et al., 2023), urban areas in the United States (Jen et al., 2016; Smith et al., 2010),
47 European cities (Brean et al., 2020), a high altitude site (Bianchi et al., 2016), and the Arctic and
48 Antarctic (Beck et al., 2021; Brean et al., 2021; Jokinen et al.; Köllner et al., 2017). However,
49 global models cannot simulate urban NPF processes currently because of the lack of amine
50 emission inventories in models.

51 Ammonia and amines also contribute to secondary organic aerosol (SOA) formation by
52 condensation of oxidation products formed by reactions with ozone, OH, or NO₃ radicals and
53 produce light-absorbing particles (Erupe et al., 2010; Malloy et al., 2009; Silva et al., 2008;
54 Nielsen, 2016; Nielsen et al., 2012; Qiu and Zhang, 2013). As a result, reducing ammonia
55 emissions has been identified as a cost-effective way to mitigate ambient fine particle
56 concentrations (Gu et al., 2021).

57 Fast-response measurements of ammonia and amines at atmospheric concentrations are very
58 challenging (Lee, 2022), although such measurements are necessary because these reduced
59 nitrogen compounds have relatively short atmospheric lifetimes (Nielsen et al., 2012). Previously,
60 (Schwab et al., 2007) made an intercomparison of six different ammonia detection methods in the
61 laboratory and found a large variance in the measured concentrations and vastly different response
62 times (over several hours) within different instruments. Difficulties in the detection of base
63 compounds also arise because these “sticky” compounds can rapidly adsorb and desorb on/from
64 the surfaces of sampling inlets to cause background signals that vary depending on ambient
65 concentrations, air humidity, and other atmospheric conditions. Thus frequent, in situ
66 measurements of instrument background signals using proper zero gases are required, especially
67 for field observations with rapidly changing ambient concentrations of base compounds.

68 Chemical ionization mass spectrometers (CIMS) using ion reagents such as protonated ethanol,
69 acetone, and water ions can detect ammonia and amines in the atmosphere with fast response
70 (Nowak et al., 2006; Benson et al., 2010; Yu and Lee, 2012 ; Hanson et al., 2011; Jen et al., 2016;
71 Nowak et al., 2010). As summarized in Table 1, CIMS technique has been used for the detection
72 of ambient ammonia and amines at a polluted site in Ohio (You et al., 2014; Yu and Lee, 2012),
73 a rural Alabama forest (You et al., 2014), and polluted urban sites in China (Zheng et al., 2015;
74 Wang et al., 2020a; Wang et al., 2016; Zhu et al., 2022). As shown in Table 1, there are even fewer
75 studies that simultaneously measured ammonia and amines. The CIMS using ethanol reagent can
76 measure amines at or below single-digit pptv concentrations with a time response of 1 minute and
77 measure simultaneously amines and ammonia (You et al., 2014; Yu and Lee, 2012 ; Erupe et al.,
78 2011; Benson et al., 2010). The CIMS using protonated water ions (i.e., proton-transfer chemical
79 ionization mass spectrometer, PTR-CIMS) can measure mono- and di-amines (Hanson et al., 2011;
80 Jen et al., 2016). Using a high-resolution time-of-flight (HR-TOF) detector coupled to CIMS (HR-
81 TOF CIMS) (with ethanol reagent), (Yao et al., 2016) measured various amines and amides in
82 Shanghai. However, isomers of amines were still not resolved in the detection; for example, the
83 measured C₂-amines still contained dimethylamine and ethylamine. Thus, a major disadvantage
84 of a mass spectrometer (regardless of mass resolution) is the inability to resolve/identify isomers.
85 To resolve isomers, tandem MS/MS analysis or an additional independent separation method (such
86 as chromatography) coupled to the mass spectrometer is necessary.

87 In situ measurements of ammonia have been made in various atmospheric environments also
88 with optical techniques such as open-path absorption (Miller et al., 2014), closed-path absorption
89 (Griffith and Galle, 2000; Ellis et al., 2010; Mcmanus et al., 2010; Leen et al., 2013; Pollack et al.,
90 2019), cavity ring-down spectroscopy (Martin et al., 2016), and photoacoustic spectroscopy

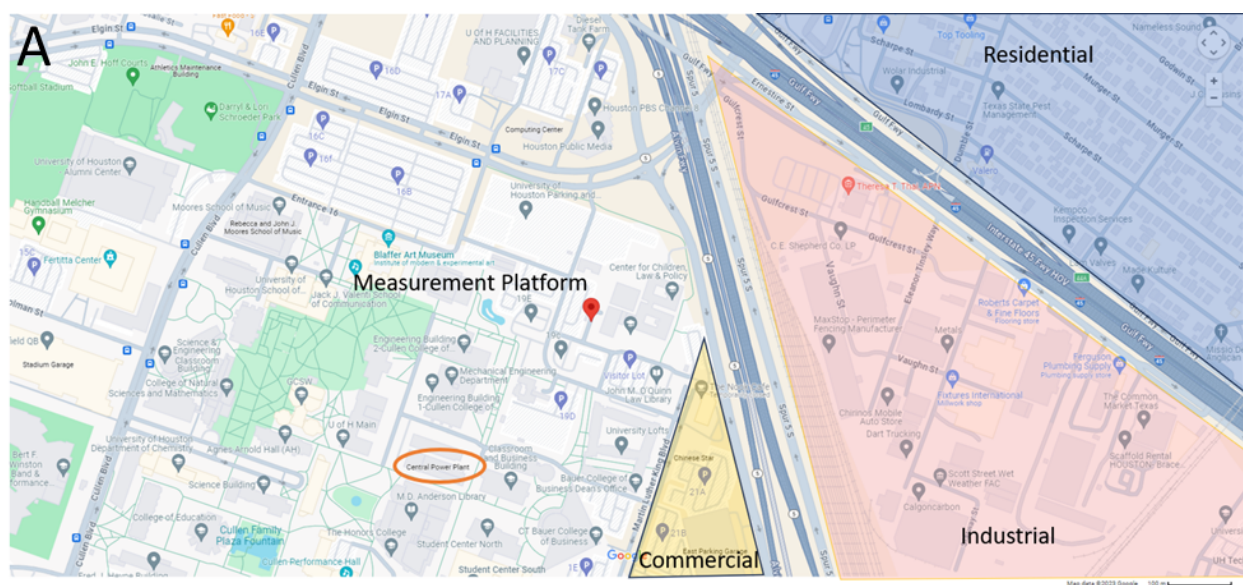
91 (Pushkarsky et al., 2002). These fast-response optical techniques were used for flux and aircraft
92 measurements of ammonia.

93 We measured ammonia and C1-C6 amines with an ethanol CIMS in October 2022 at the urban
94 center in Houston, Texas. Houston is the fourth most populated urban center in the U.S. and
95 contains a diverse range of pollutant emissions from urban activity, traffic, ship channels, oil
96 production, marine air masses, and agricultural activity. The primary goal of these measurements
97 is to quantify ammonia and C1-C6 amines in an urban setting and identify the atmospheric
98 conditions that affect their abundance. The study is amongst very few observations of ammonia
99 and amines at highly polluted urban sites in the U.S. We also compare observations in Houston
100 with previous measurements taken with the same instrument in Kent, Ohio (less polluted) (You et
101 al., 2014) and establish a quantitative relationship between ammonia and dimethylamine in a
102 different range of polluted conditions. This relationship will allow global models to simulate urban
103 NPF processes using the existing ammonia emission inventories.

104

105 2. Methods

106



107

108

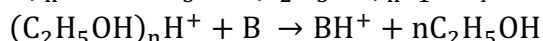
109 **Figure 1.** Location of the measurement platform, indicated by a red pin in the center of the map.
110 Nearby commercial, industrial, and residential areas are labeled by yellow, red, and blue shaded
111 sections, respectively. The nearby University of Houston power plant is circled in orange to the
112 southwest of the measurement platform. The map of the greater Houston urban area, as well as
113 the satellite view of the nearby vicinity of the measurement site, are shown in Figure S1.

114

115 The field observation took place in Houston continuously from the 8th to the 27th of October in
116 2022. Measurements were made at a stationary platform located on the campus of the University
117 of Houston (29.72° N, 95.34° W) ~2.5 km from central downtown Houston. Maps of the
118 measurement site (Figures 1 and S1). The measurement platform was located ~5 m from an active

119 parking lot, ~200 m from a low-traffic road, ~300 m from a high-traffic thoroughfare, and ~500 m
120 from an interstate highway. The immediate vicinity of the site was the University of Houston
121 campus, containing classroom buildings, dormitories, facilities services, and dining halls. Nearby
122 to the southeast of the site were several restaurants as well as an industrial park containing sites of
123 chemical supply companies, construction, machining services, and automobile shops. The site was
124 surrounded by residential areas to the south, northeast, and west. The city center and highest
125 population densities were to the northeast of the measurement site.

126
127 The ethanol CIMS instrument used has been described in detail previously (Benson et al.,
128 2010; You et al., 2014; Yu and Lee, 2012). The CIMS draws 10 standard liter per minute (slpm)
129 of sample air into a low-pressure ion-molecule region (about 2,000 Pa) where the flow mixes with
130 a pure nitrogen flow with a 2 slpm through a stainless-steel vessel of 200-proof ethanol, followed
131 by a ^{210}Po radiation source. Ammonia and amines were detected with the following ion-molecule
132 reactions based on (Erupe et al., 2011), (Yu and Lee, 2012), and (Nowak et al., 2006):



133
134 Here, “B” refers to amines, and “n” is the number of reagent ions measured by the CIMS (n=1-3).
135 The $(C_2H_5OH)_2H^+$ (m/z = 93) peak was the highest among the three reagent ions (m/z = 47, 93,
136 and 140). As shown in Figure S2, the production ions of amines were protonated ions: C1-amine
137 (m/z = 32), C2 (m/z = 46), C3 (m/z = 60), C4 (m/z = 74), C5 (m/z = 88), and C6 (m/z = 102).
138 Ammonia product ions were NH_4^+ (m/z = 18, higher peak) and $(C_2H_5OH)NH_4^+$ (m/z = 64, lower
139 peak); these two ions were strongly correlated to each other during the ammonia calibration and
140 ambient measurements, indicating they represent ammonia signals.

141
142 To obtain a background signal, the CIMS is operated with 10 minutes of sampling followed
143 by 10 minutes of background measurements. Figure S2 shows the main reagent and base
144 compound product ions during the switching between ambient and background measurements.
145 Background measurements were taken by switching a 3-way valve to supply the inlet with a flow
146 of zero air through a silicon phosphate medium (Pan Tech, Texas) to scrub ammonia and amines.
147 The reagent signal was taken as the sum of three ethanol reagent ions. Reagent ion signals were
148 typically around 400 kHz with less than 10 % difference between ambient and background
149 measurement modes. Ammonia and amine concentrations were calculated by the difference
150 between the ambient and background signals normalized to 1,000,000 Hz of reagent ion signal
151 multiplied by a calibration factor. Calibration of the instrument was carried out with diluted
152 ammonia in nitrogen and permeation tubes of methylamine, dimethylamine, trimethylamine,
153 diethylamine, and diisopropylamine (Kin-tek, USA). Due to the difficulty of obtaining a
154 calibration standard, C5 amines were assumed to have the same sensitivity as C6 amines. The
155 calibration factors for each compound and detection limits were found to be similar to the results
156 from the calibration of the instrument by (You et al., 2014) (Table S1), over a period of nearly 10
157 years, demonstrating an excellent reproducibility in the instrument performance. The time
158 response of the CIMS instrument to ammonia and amines is defined as where the signal stabilizes

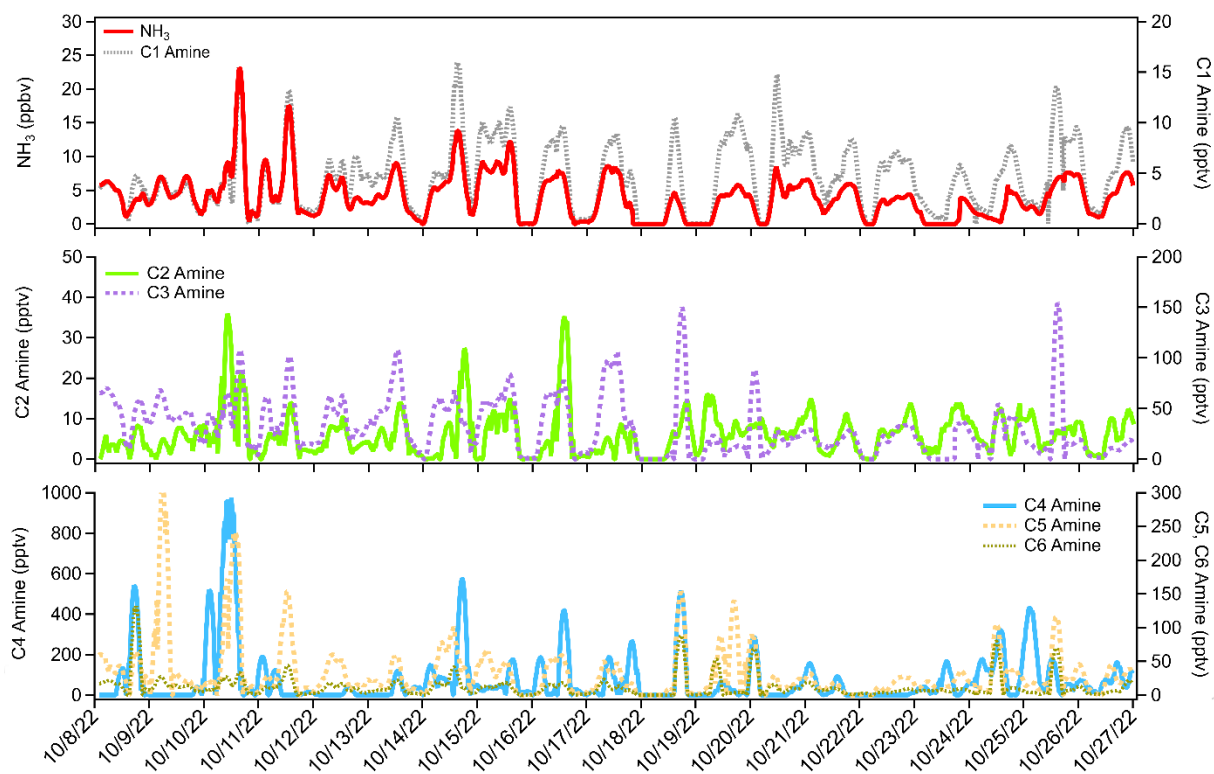
159 at its “double e-folded” concentration of $1/e^2$ during the calibration. Average response times for
160 ammonia and amines were smaller than 1 minute. For each 10-minute cycle of background and
161 measurement, the first two minutes of each background/measurement cycle were excluded from
162 the data analysis to allow the instrument to reach a steady concentration.

163 The uncertainty in the CIMS included error in the permeation sources, which ranged from 2%
164 to 5% depending on the compound. The permeation sources were diluted in two stages using flow
165 controllers that each had uncertainties of 1.5%. Total error in the calibration of the CIMS was
166 6.7%. Overall uncertainty in the CIMS was 30%, accounting for calibration error, variability of
167 ion signals, and inlet losses.

168 Meteorological data was measured concurrently on the platform by a Vaisala HMP-45c for
169 temperature and relative humidity, and a RM Young 05305 wind speed and direction sensor.
170 Additionally, CO and NO_x (NO+NO₂) were measured with Thermo 48c and Thermo 42c-TL,
171 respectively. These measurements were provided by the University of Houston. The uncertainty
172 in trace gas (CO and NO_x) measurements arises from instrumental uncertainty in the Thermo 48c
173 CO analyzer and Thermo 42c-TL NO_x analyzer. Zero correction was performed on this instrument
174 daily by switching to a flow of zero air. The typical uncertainty of each of these instruments was
175 5%.

176
177
178
179

3. Results and Discussion

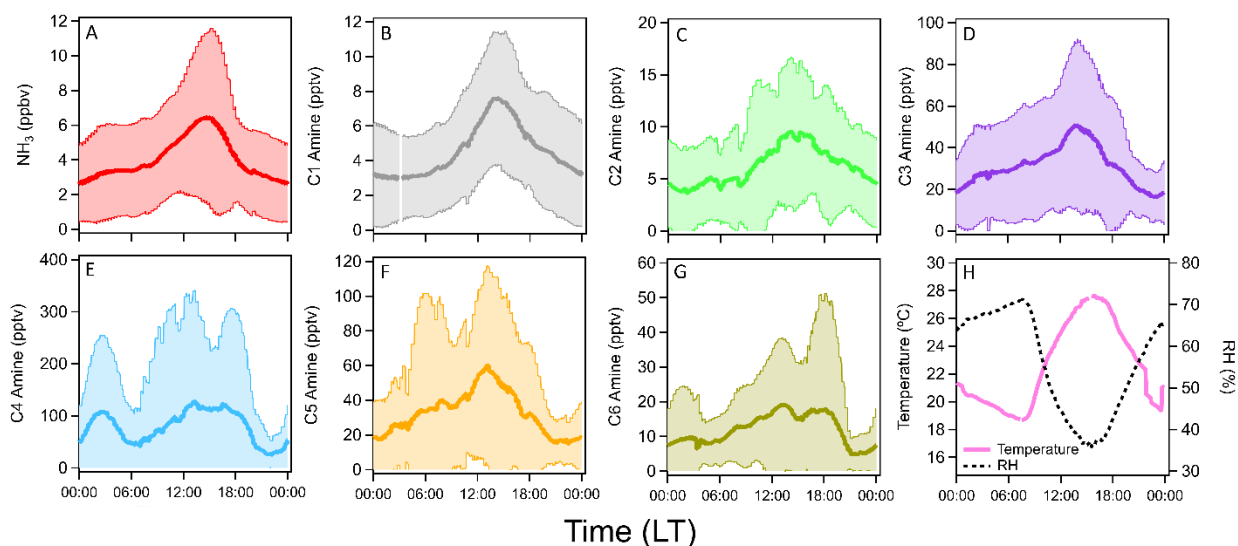


180

181 **Figure 2.** Time series of ammonia and C1-C6 amines observed at the urban center in Houston,
182 Texas, in October 2022.

183 The time series of ammonia and amines during the ambient measurement period is shown in
184 Figure 2. The average ammonia concentration during the measurement campaign was 4 ppbv with
185 several short-term spikes above 10 ppbv and one occasion when the concentration exceeded 20
186 ppbv. Concentrations of C1 amine averaged 4 pptv with several spikes up to 15 pptv. Average C2
187 amine concentrations were 6 pptv with frequent but brief periods of concentrations more than 10
188 pptv. Average C3 amine concentrations were 31 pptv with brief increases in concentration above
189 100 pptv. C4 amine was the most abundant amine observed during the measurement period with
190 an average concentration of 79 pptv with spikes in concentration into the hundreds of pptv.
191 Average C5 and C6 amine concentrations were 33 and 12 pptv, respectively. These concentrations
192 in Houston were generally consistent with concentrations measured in other urban sites (Table 1).
193 Previous CIMS ammonia measurements from aircraft flights above Houston observed similar
194 baseline concentrations of ammonia (0.2-3 ppbv) with brief spikes in concentration (up to 80 ppbv)
195 associated with agricultural or industrial activity (Nowak et al., 2010). Additionally, ammonia
196 concentrations of similar magnitude to the high spikes in concentration observed in this study have
197 been reported in Shanghai (Xiao et al., 2015) as well as an urban site in Romania (Petrus et al.,
198 2022), with high ammonia concentrations corresponding to high temperatures and high traffic
199 activity. Long-term measurements taken in Nanjing with a cavity ring-down spectrometer also
200 showed an average ammonia concentration of 12 ppbv (Liu et al., 2024). Measurements of amines
201 in Atlanta, Georgia showed <1 to 3 pptv concentrations of C1 and C2 amines, and C3 and C6
202 amines up to 15-25 pptv (Hanson et al., 2011). Yao et al. (Yao et al., 2016) measured amines at
203 the level of pptv or sub-pptv, e.g., C2 amines of 3.9 ± 1.2 pptv, in urban Shanghai during the
204 summer. It is possible that measured concentrations of amines measured here contain some
205 interference from amides formed from oxidation of emitted amines. The CIMS does not have
206 sufficient resolving power to separate trimethylamine (m/z 59.11) from acetamide (m/z 59.07), for
207 example. Therefore, these amine concentrations represent an upper limit of amine concentrations
208 (assuming all of the detected signal is due to the presence of amines). However, (Yao et al., 2016)
209 measured amide concentrations in urban Shanghai in the tens to hundreds of pptv, while C1-C2
210 amine concentrations in Shanghai were similar to Houston observations reported here. Considering
211 the consistency between amine measurements at these two urban locations, it is likely that
212 interference from amides in the CIMS was minimal for C1 and C2 amines. The discrepancies
213 between these two urban areas become more pronounced for C3-C6 amines (Table 1), which
214 makes amide interference a possible explanation for elevated concentrations of C3 amines and
215 above.

216



217

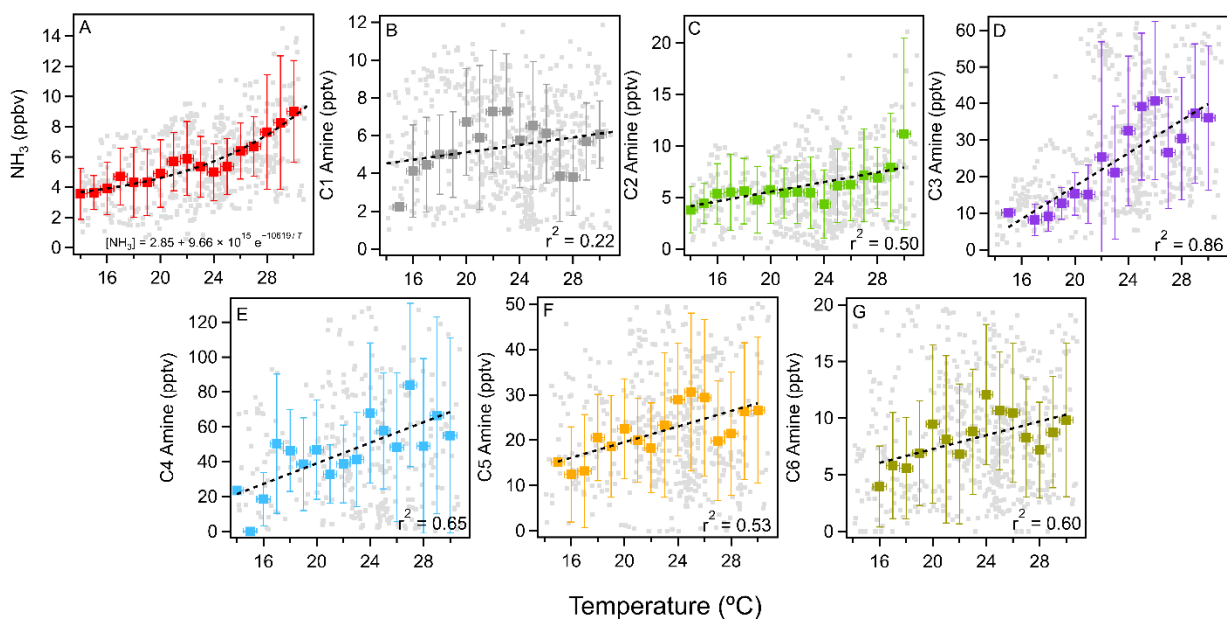
218 **Figure 3.** Averaged diurnal cycles of (a) ammonia, (b-g) C1-C6 amines, (h) temperature, and RH
 219 in Houston, Texas, during the observation period (19 days continuously). Shaded areas indicate 1
 220 standard deviation from the mean values of observation data.

221 Figure 3 shows the averaged diurnal concentrations of ammonia and amines during the
 222 observation period. Ammonia and amines had a diurnal cycle with peak concentrations in the
 223 afternoon with higher ambient temperatures. Generally, ammonia and amines correlated with one
 224 another throughout the measurement campaign, while C1-C3 amines showed the highest
 225 correlation with ammonia. Peak concentrations of all compounds corresponded with the high
 226 temperature of the day at around 3 pm local time. This was especially pronounced for ammonia,
 227 C1 and C3 amines. The relationships between ammonia and amines and temperature are shown in
 228 Figure 4. Ammonia had the strongest correlation with temperature, and the relationship fit an
 229 exponential parameterization, as the following:

230
$$[NH_3] = 2.85 + 9.66 \times 10^{15} e^{-\frac{10619}{T}}$$

231 Amines generally showed linear relationships with temperature, with C3 and C4 amines displaying
 232 the strongest relationships. C3 amines increased by 2.3 pptv per °C ($r^2 = 0.86$) and C4 by 2.9 pptv
 233 per °C ($r^2 = 0.65$). C5 and C6 amines were also moderately correlated with temperature, increasing
 234 by 1.2 pptv per °C and 0.5 pptv per °C, respectively ($r^2 = 0.60$ for both C5 and C6). On the other
 235 hand, the correlation of C1 and C2 amines with temperature were weaker: C1 only increased by
 236 0.1 pptv per °C with almost no correlation ($r^2 = 0.22$), and C2 increased by 0.8 pptv per °C ($r^2 =$
 237 0.50). The temperature dependence of ammonia and amines was previously observed in a rural
 238 forest in Alabama by (You et al., 2014), which attributed this partially to particle-to-gas conversion
 239 of ammonia and amine containing particles at elevated temperatures. The temperature dependence
 240 could also be due to higher emissions at higher temperatures. The temperature dependence of
 241 ammonia and amines has been observed at other urban, suburban and rural locations such as Kent,

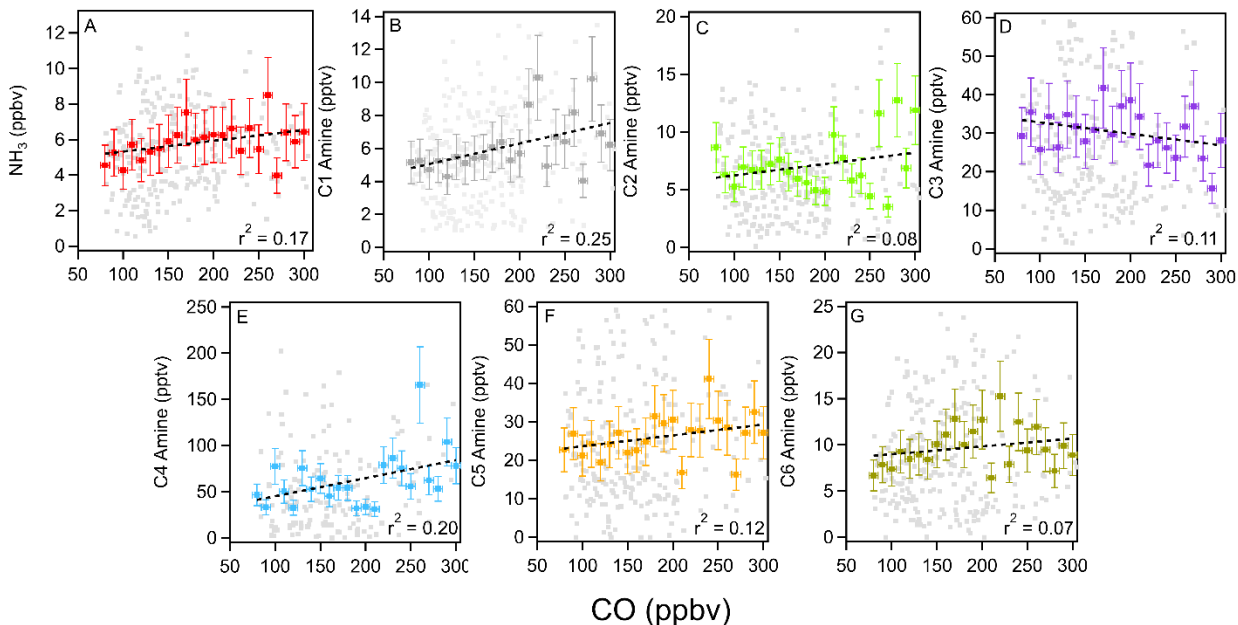
242 Ohio (You et al., 2014), Atlanta (Hanson et al., 2011), Delaware (Freshour et al., 2014), the
 243 Southern Great Plains (Freshour et al., 2014), and rural central Germany (Kürten et al., 2016).
 244



245
 246

247 **Figure 4.** Temperature dependence of (a) ammonia and (b-g) C1-C6 amines measured in Houston.
 248 Vertical bars indicate 1 standard deviation from the mean values of observation data. Binned
 249 temperatures are shown in colored squares, 1-minute averaged data is shown in gray squares.
 250 Horizontal bars indicate bin width. Black dashed lines indicate exponential fit for ammonia and
 251 linear fits for amines.

252 Anthropogenic pollutants such as CO and NO_x and CO can serve as tracers for industrial and
 253 traffic activities. Ammonia and amines in general showed a positive correlation with CO, with the
 254 exception of C3 amines (Figure 5). As ammonia, amines, and CO can be traced to traffic or
 255 industrial emissions, the positive relationship between these compounds implies that these base
 256 compounds were emitted from pollutant sources. Unlike with CO, there was a negative correlation
 257 with NO_x (Figure S3). This lack of a strong correlation between NO_x and ammonia was previously
 258 observed in Nanjing where a strong reduction in NO_x concentration during COVID-19 lockdown
 259 periods was not accompanied by an equivalent reduction in ammonia concentrations (Liu et al.,
 260 2024). This may indicate some unique emission sources for ammonia and amines that do not co-
 261 emit NO_x.
 262

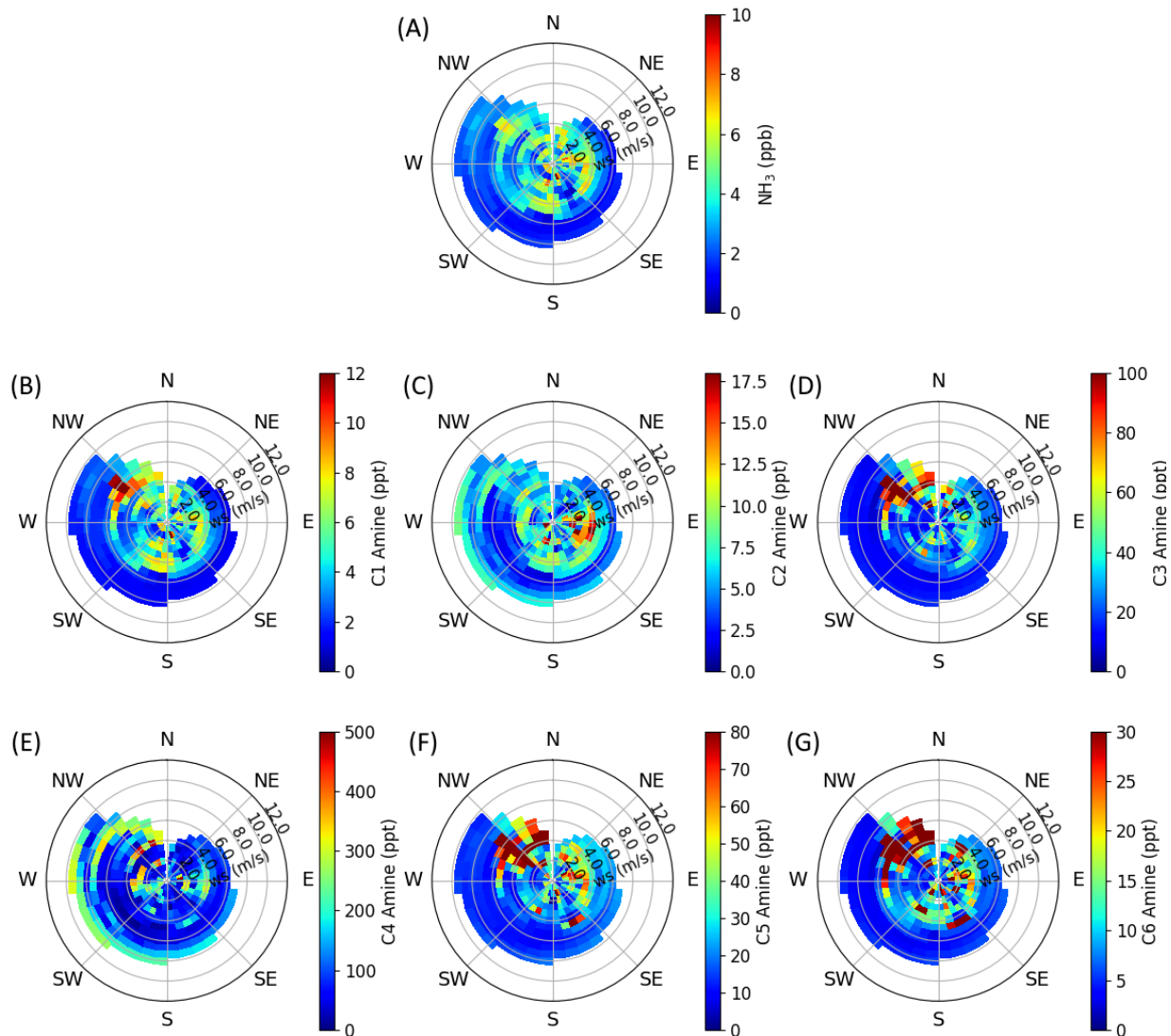


263
 264 **Figure 5.** Correlation between ammonia (a) and C1-C6 amines (b-g) with the collocated CO
 265 concentrations during the measurement campaign. Binned CO concentrations are shown in colored
 266 squares, 5-minute averaged data shown in gray squares. Vertical bars indicate 1 standard deviation
 267 from the mean values of observation data. Horizontal bars indicate bin widths. Black dashed lines
 268 indicate linear fits.

269 Wind speed and direction can help to identify local sources of ammonia and amines near the
 270 measurement site. Figures 6 and S4 show the correlation of ammonia and amines with wind speeds
 271 and direction throughout the observation period. Consistent between all base compounds is the
 272 high concentration coming from the southeast. This is the direction of the interstate highway,
 273 industrial areas, and train yards (Figures 1 and S1). Ammonia and most amines also have a
 274 pronounced source from the northwest – this is the direction of downtown Houston, where
 275 population density is highest. Except for C2 and C4 amines, the observed ammonia and amines in
 276 Houston were higher during periods of low wind speeds. The abundant C2 and C4 at high wind
 277 speeds may suggest that C2 and C4 amines were transported from more distant sources.

278 Figure S5 shows the average diurnal cycle of ammonia and amines on weekdays as opposed
 279 to weekends. Except for C2 and C4 amines, there was a clear decrease in concentrations during
 280 weekends during the afternoon peak. Weekends saw much less traffic and activity on the
 281 University of Houston campus. During this observation period, ambient temperatures were higher
 282 during the weekends, which would increase emissions. Therefore, the differences in weekdays vs.
 283 weekends indicate that amines and ammonia were indeed emitted from traffic and industrial
 284 activities. Lower average amine concentrations on weekends were also observed during mobile
 285 measurements in Yangtze River Delta cities (Chang et al., 2022).

286
 287



288
289

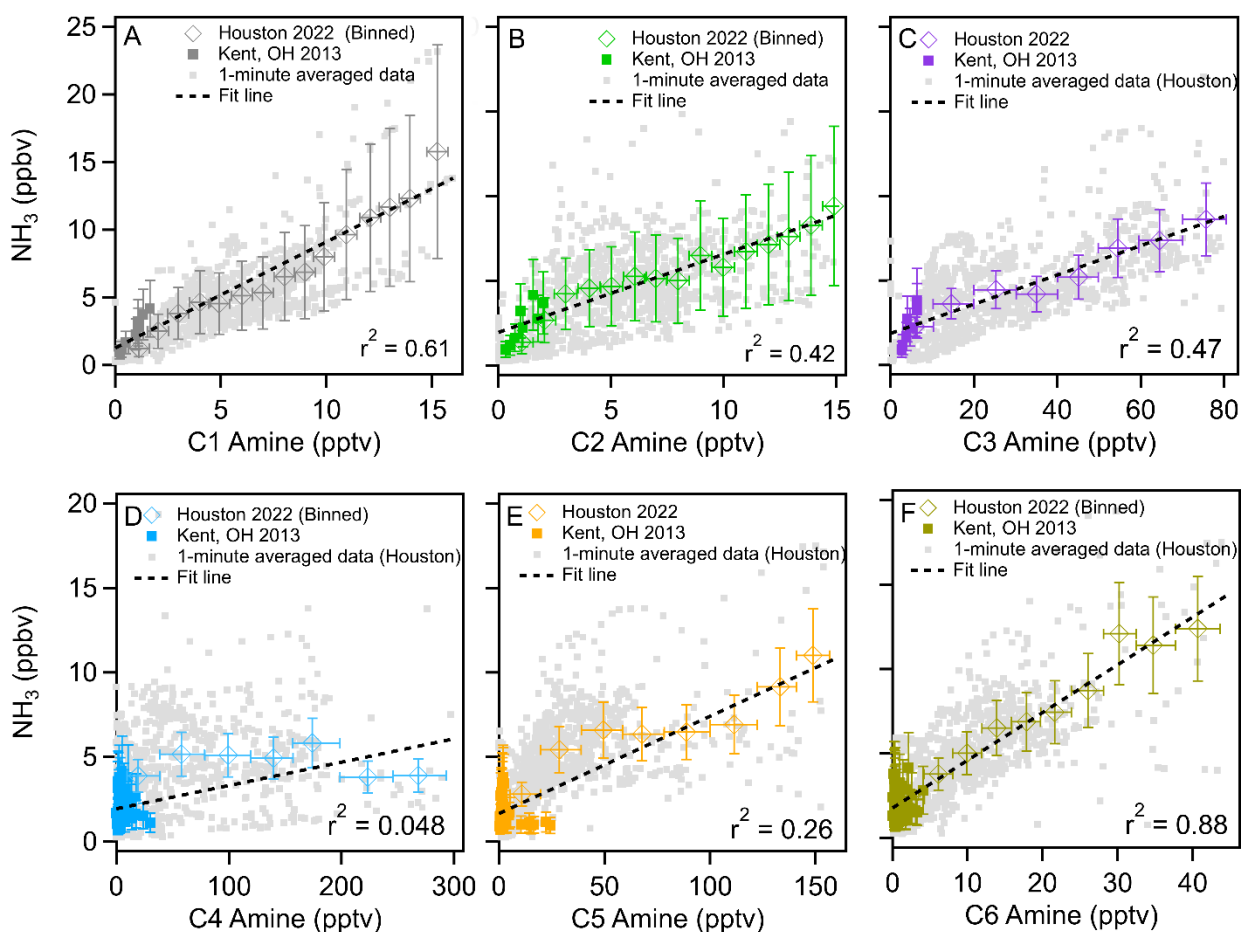
290 **Figure 6.** Wind rose plots of (a) ammonia and (b-g) C1-C6 amines observed in urban Houston.
291 The color scale indicates concentration, and radial intensity shows wind speed.

292
293
294

4. Atmospheric Implications

295 Field observations show that sulfuric acid and amines are responsible for aerosol nucleation
296 (Yao et al., 2016; Yan et al., 2021; Cai et al., 2021; Cai et al., 2023; Jen et al., 2016; Smith et al.,
297 2010; Brean et al., 2020), however, currently, global models do not have amine emission
298 inventories. Figure 7 shows the correlation of ammonia with C1-C6 amines measured during this
299 campaign. This figure also includes that data obtained with the same instrument in Kent, Ohio,
300 (You et al., 2014). It is clear from this figure that concentrations of ammonia, C1, C2, C3, C5, and
301 C6 amines were positively correlated with one another throughout the study: r^2 values for the
302 correlation between ammonia and amines were 0.61 for C1, 0.42 for C2, 0.47 for C3, 0.26 for C5

303 and 0.88 for C6. These relationships imply that these compounds are mostly co-emitted from
 304 similar sources and undergo similar atmospheric transport. C4 amines showed no correlation with
 305 ammonia and lower-mass amines – the r^2 value for C4 vs. NH_3 was 0.048. This indicates a unique
 306 source for C4 amines, consistent with both elevated C4 concentrations at high wind speeds and
 307 higher weekend C4 concentrations as discussed previously. Correlations of C1-C3 amines
 308 concentrations, taken from the linear fits of the plots shown in Figure 7, were approximately
 309 equivalent to $1.1 \times 10^{-3} [\text{NH}_3]$, $1.4 \times 10^{-3} [\text{NH}_3]$, and $8.4 \times 10^{-3} [\text{NH}_3]$, respectively. C5 and C6
 310 amine concentrations were $1.9 \times 10^{-2} [\text{NH}_3]$ and $3.5 \times 10^{-3} [\text{NH}_3]$, respectively (Table S2). From
 311 these results, we propose that global modelers use 0.1 % of the ammonia concentration as a proxy
 312 of dimethylamine to simulate urban NPF processes. However, this recommendation comes with
 313 the caveat that measured C2 amines may include dimethylamine as well as ethylamine due to the
 314 inability of mass spectrometry to resolve isomers. Therefore, this correlation represents only the
 315 upper bound of dimethylamine concentrations.
 316



317
 318 **Figure 7.** Correlations of C1-C6 amines with ammonia throughout the observation period in
 319 Houston (diamonds) and Kent, OH (squares) as reported by (You et al., 2014). Binned
 320 concentrations are shown in colored squares, 1-minute averaged data from Houston are shown in

321 gray squares. Vertical bars indicate one standard deviation from the mean values of observation
322 data. Horizontal bars indicate bin widths. Black dashed lines indicate linear fits of the combined
323 data from Kent and Houston.

324 From these observations made in very polluted Houston and less polluted Kent, we propose
325 that at the polluted sites in the United States, dimethylamine concentrations can be estimated using
326 the proxy, 0.1% ammonia concentrations. The caveat of this proxy is that it is based on only two
327 locations in the United States and did not consider different emission sectors. There has been so
328 far only one attempt to use quantify the aerosol nucleation processes using sulfuric acid and
329 dimethylamine in the global model by Zhao et al. (Zhao et al., 2024) and they concluded that this
330 nucleation process is dominant globally in polluted boundary layer, from China, India, Europe to
331 United States. In this cited study the authors used the proxy of dimethylamine using ammonia
332 concentrations, for example, dimethylamine/ammonia ratio of 0.0070, 0.0018, and 0.0100, for
333 chemical industrial, other industrial, and residential sources; these proxies were derived by Mao
334 et al. (Mao et al., 2018) based on the measurement made in Nanjing (Zheng et al., 2015). Our
335 observations indicate that (Zhao et al., 2024) likely overestimated dimethylamine concentrations
336 for polluted sites in the United States overall, and thus overpredicted nucleation rates as well. Thus,
337 our results can provide more constrained proxy for polluted sites in the United States for future
338 modeling studies.

339 **5. Conclusions**

340 Our observations in urban Houston show that ammonia and amines generally followed a clear
341 diurnal cycle, peaking in the early afternoon when the ambient temperature was highest during the
342 day. We found a correlation between ammonia/amines and ambient temperature. The diurnal
343 cycles and temperature dependence of these compounds are consistent with (You et al., 2014)
344 which showed that the gas-to-particle conversion contributes to the temperature dependence. To
345 verify this process, the chemical composition of particle is needed, but particle measurements were
346 not available during the present study. Additionally, the observed temperature dependence could
347 be due to increased emissions of ammonia and amines from biogenic and anthropogenic sources.
348 On the other hand, photochemical aging that occurs typically during the higher solar flux can also
349 reduce the gas phase amines at the noontime; thus, photochemical aging was unlikely the main
350 driving factor to produce higher concentrations of amines around noon.

351 High concentrations of ammonia and amines were correlated with local air masses from
352 densely populated areas and areas of high traffic, industry, and other human activity. This suggests
353 that most ammonia and amines measured in Houston originated from pollutant sources, consistent
354 with the correlation observed with CO concentrations. There was also a clear increase in ammonia
355 and amines on days with more human activity as shown by the results of concentrations on
356 weekends vs weekdays. We observed a consistent relationship between ammonia and amines
357 during our measurement campaign as well as with observations in less densely populated Kent,
358 Ohio, suggesting that it is reasonable to parameterize amine emission inventories based on existing
359 ammonia inventories to simulate urban NPF processes. However, as the CIMS is incapable of

360 resolving amides or isomers, this parameterization is only capable of representing the upper
361 bounds of amines. Further work involving instrumentation capable of isomer resolution such as
362 tandem MS/MS or chromatographic separation is needed to determine typical isomer ratios of
363 amines for more accurate parameterizations.

364 Measuring ammonia and amines in the atmosphere is one of the most challenging areas in the
365 development of atmospheric analytical instruments (Lee, 2022; Lee et al., 2019). The CIMS used
366 in this campaign is currently one of the few instruments in the world that is capable of simultaneous
367 measurements of ammonia and amines at atmospherically relevant detection limits and timescales.
368 Very importantly, our CIMS, despite its relatively low mass resolution, has measured ammonia
369 and amines at various atmospheric conditions, ranging from the rural forests (You et al., 2014;
370 Kanawade et al., 2014), a relatively less polluted site (Yu and Lee, 2012 ; You et al., 2014; Erupe
371 et al., 2010), to the extremely polluted urban environment (this study), with consistent instrument
372 sensitivities over the decade; to our knowledge, this is the only instrument that demonstrated such
373 consistency in the performance. Studies have shown that the co-presence of ammonia and amines
374 can enhance sulfuric acid nucleation rates compared to ammonia alone (Yu et al., 2012; Glasoe et
375 al., 2015; Myllys et al., 2019). From this perspective, simultaneous measurements of ammonia and
376 amines will be required for the correct prediction of NPF processes in the atmosphere.
377 Measurements of ammonia and amines with comprehensive calibration as shown in the present
378 study are very even rarer, but such measurements are needed for mitigating urban air quality
379 problems and the health effects of ultrafine particles.

380

381 **Author Contributions**

382 SHL designed the research; LT and SHL performed measurements; JF provided the measurement
383 platform as well as the trace gas and meteorology data; LT and SHL wrote the manuscript.

384 **Competing interests**

385 The authors declare that they have no conflict of interest.

386 **Acknowledgements**

387 We acknowledge funding support from National Science Foundation (grant numbers 2209722,
388 2117389, and 2107916) and Texas Commission on Environmental Quality (grant number 582-22-
389 31535-018).

390

391 **Table 1.** Ammonia and amine measurements with CIMS at various locations reported in the
 392 literature. DL, detection limit of each instrument.

Location	NH ₃ (ppbv)	C1 Amine (pptv)	C2 Amine (pptv)	C3 Amine (pptv)	C4 Amine (pptv)	C5 Amine (pptv)	C6 Amine (pptv)
Rural Alabama Forest (You et al., 2014)*	Up to 1-2	< DL	< DL	1 - 10	< DL	< DL	< DL
Kent, Ohio (You et al., 2014)*	Up to 6	1 – 4	< DL	5 - 10	10 - 50	10 - 100	< DL
Kent, Ohio (Yu and Lee, 2012)*	0.5 ± 0.26	-	8 ± 3	16 ± 7	-	-	-
Atlanta, Georgia (Hanson et al., 2011)†	-	< 1	3	4 – 15	25	-	-
Lewes, Delaware (Freshour et al., 2014)†	0.8	5	28	6	150	1	2
Lamont, Oklahoma (Freshour et al., 2014)†	0.9	4	14	35	150	98	20
Minneapolis, Minnesota (Freshour et al., 2014)†	1.8	4	42	19	14	20	5
Shanghai (Yao et al., 2016)‡	-	3.9 ± 1.2	6.6 ± 1.2	0.4 ± 0.1	3.6 ± 1.0	0.7 ± 0.3	1.8 ± 0.8
Nanjing (Zheng et al., 2015)‡	1.7 ± 2.3	7.2 ± 7.4 (C1 + C2 + C3)			-	-	-
Wangdu	-	-	14.6 ± 14.9	-	-	-	-

(Wang et al., 2020b)§							
Beijing (Zhu et al., 2022)‡	2.8 ± 2.0	5.2 ± 4.3 (C1 + C2 + C3)	-	-	-		
Houston, TX (This study)*	4 ± 1	4 ± 2	6 ± 2	31 ± 9	79 ± 30	33 ± 12	12 ± 4

393

394 * CIMS with ethanol reagent

395 † Proton-transfer chemical ionization mass spectrometer (PTR-CIMS)

396 ‡ High-resolution time of flight chemical ionization mass spectrometer (HR-TOF CIMS) with
397 ethanol reagent

398 § Vocus proton transfer time-of-flight mass spectrometer (PTR-TOF MS)

399

400

401 **References**

- 402
- 403 Almeida, J., Schobesberger, S., Kürten, A., Ortega, I. K., Kupiainen-Määttä, O., Praplan, A. P.,
 404 Adamov, A., Amorim, A., Bianchi, F., Breitenlechner, M., David, A., Dommen, J.,
 405 Donahue, N. M., Downard, A., Dunne, E., Duplissy, J., Ehrhart, S., Flagan, R. C.,
 406 Franchin, A., Guida, R., Hakala, J., Hansel, A., Heinritzi, M., Henschel, H., Jokinen, T.,
 407 Junninen, H., Kajos, M., Kangasluoma, J., Keskinen, H., Kupc, A., Kurtén, T., Kvashin,
 408 A. N., Laaksonen, A., Lehtipalo, K., Leiminger, M., Leppä, J., Loukonen, V.,
 409 Makhmutov, V., Mathot, S., McGrath, M. J., Nieminen, T., Olenius, T., Onnela, A.,
 410 Petäjä, T., Riccobono, F., Riipinen, I., Rissanen, M., Rondo, L., Ruuskanen, T., Santos,
 411 F. D., Sarnela, N., Schallhart, S., Schnitzhofer, R., Seinfeld, J. H., Simon, M., Sipilä, M.,
 412 Stozhkov, Y., Stratmann, F., Tomé, A., Tröstl, J., Tsagkogeorgas, G., Vaattovaara, P.,
 413 Viisanen, Y., Virtanen, A., Vrtala, A., Wagner, P. E., Weingartner, E., Wex, H.,
 414 Williamson, C., Wimmer, D., Ye, P., Yli-Juuti, T., Carslaw, K. S., Kulmala, M., Curtius,
 415 J., Baltensperger, U., Worsnop, D. R., Vehkamäki, H., and Kirkby, J.: Molecular
 416 understanding of sulphuric acid–amine particle nucleation in the atmosphere, *Nature*,
 417 502, 359-363, 10.1038/nature12663, 2013.
- 418 Beck, L. J., Sarnela, N., Junninen, H., Hoppe, C. J. M., Garmash, O., Bianchi, F., Riva, M., Rose,
 419 C., Peräkylä, O., Wimmer, D., Kausiala, O., Jokinen, T., Ahonen, L., Mikkilä, J., Hakala,
 420 J., He, X.-C., Kontkanen, J., Wolf, K. K. E., Cappelletti, D., Mazzola, M., Traversi, R.,
 421 Petroselli, C., Viola, A. P., Vitale, V., Lange, R., Massling, A., Nøjgaard, J. K., Krejci,
 422 R., Karlsson, L., Zieger, P., Jang, S., Lee, K., Vakkari, V., Lampilahti, J., Thakur, R. C.,
 423 Leino, K., Kangasluoma, J., Duplissy, E.-M., Siivola, E., Marbouti, M., Tham, Y. J.,
 424 Saiz-Lopez, A., Petäjä, T., Ehn, M., Worsnop, D. R., Skov, H., Kulmala, M., Kerminen,
 425 V.-M., and Sipilä, M.: Differing Mechanisms of New Particle Formation at Two Arctic
 426 Sites, *Geophysical Research Letters*, 48, e2020GL091334,
 427 <https://doi.org/10.1029/2020GL091334>, 2021.
- 428 Benson, D. R., Markovich, A., Al-Refai, M., and Lee, S. H.: A Chemical Ionization Mass
 429 Spectrometer for ambient measurements of Ammonia, *Atmos. Meas. Tech.*, 3, 1075-
 430 1087, 10.5194/amt-3-1075-2010, 2010.
- 431 Bianchi, F., Tröstl, J., Junninen, H., Frege, C., Henne, S., Hoyle, C. R., Molteni, U., Herrmann,
 432 E., Adamov, A., Bukowiecki, N., Chen, X., Duplissy, J., Gysel, M., Hutterli, M.,
 433 Kangasluoma, J., Kontkanen, J., Kürten, A., Manninen, H. E., Münch, S., Peräkylä, O.,
 434 Petäjä, T., Rondo, L., Williamson, C., Weingartner, E., Curtius, J., Worsnop, D. R.,
 435 Kulmala, M., Dommen, J., and Baltensperger, U.: New particle formation in the free
 436 troposphere: A question of chemistry and timing, *Science*, 352, 1109-1112,
 437 10.1126/science.aad5456, 2016.
- 438 Brean, J., Dall’Osto, M., Simó, R., Shi, Z., Beddows, D. C. S., and Harrison, R. M.: Open ocean
 439 and coastal new particle formation from sulfuric acid and amines around the Antarctic
 440 Peninsula, *Nature Geoscience*, 14, 383-388, 10.1038/s41561-021-00751-y, 2021.
- 441 Brean, J., Beddows, D. C. S., Shi, Z., Temime-Roussel, B., Marchand, N., Querol, X., Alastuey,
 442 A., Minguillón, M. C., and Harrison, R. M.: Molecular insights into new particle
 443 formation in Barcelona, Spain, *Atmos. Chem. Phys.*, 20, 10029-10045, 10.5194/acp-20-
 444 10029-2020, 2020.
- 445 Cai, R., Yin, R., Li, X., Xie, H.-B., Yang, D., Kerminen, V.-M., Smith, J. N., Ma, Y., Hao, J.,
 446 Chen, J., Kulmala, M., Zheng, J., Jiang, J., and Elm, J.: Significant contributions of

447 trimethylamine to sulfuric acid nucleation in polluted environments, *npj Climate and*
448 *Atmospheric Science*, 6, 75, 10.1038/s41612-023-00405-3, 2023.

449 Cai, R., Yan, C., Yang, D., Yin, R., Lu, Y., Deng, C., Fu, Y., Ruan, J., Li, X., Kontkanen, J.,
450 Zhang, Q., Kangasluoma, J., Ma, Y., Hao, J., Worsnop, D. R., Bianchi, F., Paasonen, P.,
451 Kerminen, V. M., Liu, Y., Wang, L., Zheng, J., Kulmala, M., and Jiang, J.: Sulfuric acid–
452 amine nucleation in urban Beijing, *Atmos. Chem. Phys.*, 21, 2457-2468, 10.5194/acp-21-
453 2457-2021, 2021.

454 Chang, Y., Wang, H., Gao, Y., Jing, S. a., Lu, Y., Lou, S., Kuang, Y., Cheng, K., Ling, Q., Zhu,
455 L., Tan, W., and Huang, R.-J.: Nonagricultural Emissions Dominate Urban Atmospheric
456 Amines as Revealed by Mobile Measurements, *Geophysical Research Letters*, 49,
457 e2021GL097640, <https://doi.org/10.1029/2021GL097640>, 2022.

458 Ellis, R. A., Murphy, J. G., Pattey, E., van Haarlem, R., O'Brien, J. M., and Herndon, S. C.:
459 Characterizing a Quantum Cascade Tunable Infrared Laser Differential Absorption
460 Spectrometer (QC-TILDAS) for measurements of atmospheric ammonia, *Atmos. Meas.*
461 *Tech.*, 3, 397-406, 10.5194/amt-3-397-2010, 2010.

462 Erupe, M. E., Viggiano, A. A., and Lee, S. H.: The effect of trimethylamine on atmospheric
463 nucleation involving H₂SO₄, *Atmos. Chem. Phys.*, 11, 4767-4775, 2011.

464 Erupe, M. E., Benson, D. R., Li, J., Young, L.-H., Verheggen, B., Al-Refai, M., Tahboub, O.,
465 Cunningham, V., Frimpong, F., Viggiano, A. A., and Lee, S.-H.: Correlation of aerosol
466 nucleation rate with sulfuric acid and ammonia in Kent, Ohio: An atmospheric
467 observation, *Journal of Geophysical Research: Atmospheres*, 115,
468 <https://doi.org/10.1029/2010JD013942>, 2010.

469 Freshour, N. A., Carlson, K. K., Melka, Y. A., Hinz, S., Panta, B., and Hanson, D. R.: Amine
470 permeation sources characterized with acid neutralization and sensitivities of an amine
471 mass spectrometer, *Atmos. Meas. Tech.*, 7, 3611-3621, 10.5194/amt-7-3611-2014, 2014.

472 Ge, X., Wexler, A. S., and Clegg, S. L.: Atmospheric amines – Part I. A review, *Atmospheric*
473 *Environment*, 45, 524-546, <https://doi.org/10.1016/j.atmosenv.2010.10.012>, 2011a.

474 Ge, X., Wexler, A. S., and Clegg, S. L.: Atmospheric amines – Part II. Thermodynamic
475 properties and gas/particle partitioning, *Atmospheric Environment*, 45, 561-577,
476 <https://doi.org/10.1016/j.atmosenv.2010.10.013>, 2011b.

477 Glasoe, W. A., Volz, K., Panta, B., Freshour, N., Bachman, R., Hanson, D. R., McMurry, P. H.,
478 and Jen, C.: Sulfuric acid nucleation: an experimental study of the effect of seven bases,
479 *J. Geophys. Res.*, 120, 1933-1950, Doi: 10.1002/2014JD022730, 2015.

480 Griffith, D. W. T. and Galle, B.: Flux measurements of NH₃, N₂O and CO₂ using dual beam
481 FTIR spectroscopy and the flux–gradient technique, *Atmospheric Environment*, 34,
482 1087-1098, [https://doi.org/10.1016/S1352-2310\(99\)00368-4](https://doi.org/10.1016/S1352-2310(99)00368-4), 2000.

483 Gu, B., Zhang, L., Van Dingenen, R., Vieno, M., Van Grinsven, H. J. M., Zhang, X., Zhang, S.,
484 Chen, Y., Wang, S., Ren, C., Rao, S., Holland, M., Winiwarter, W., Chen, D., Xu, J., and
485 Sutton, M. A.: Abating ammonia is more cost-effective than nitrogen oxides for
486 mitigating PM_{2.5} air pollution, *Science*, 374, 758-762, 10.1126/science.abf8623, 2021.

487 Hanson, D. R., McMurry, P. H., Jiang, J., Tanner, D., and Huey, L. G.: Ambient Pressure Proton
488 Transfer Mass Spectrometry: Detection of Amines and Ammonia, *Environmental Science*
489 *& Technology*, 45, 8881-8888, 10.1021/es201819a, 2011.

490 Jen, C. N., Bachman, R., Zhao, J., McMurry, P. H., and Hanson, D. R.: Diamine-sulfuric acid
491 reactions are a potent source of new particle formation, *Geophysical Research Letters*,
492 43, 867-873, <https://doi.org/10.1002/2015GL066958>, 2016.

493 Jokinen, T., Sipilä, M., Kontkanen, J., Vakkari, V., Tisler, P., Duplissy, E. M., Junninen, H.,
494 Kangasluoma, J., Manninen, H. E., Petäjä, T., Kulmala, M., Worsnop, D. R., Kirkby, J.,
495 Virkkula, A., and Kerminen, V. M.: Ion-induced sulfuric acid–ammonia nucleation drives
496 particle formation in coastal Antarctica, *Science Advances*, 4, eaat9744,
497 10.1126/sciadv.aat9744,

498 Kanawade, V. P., Tripathi, S. N., Siingh, D., Gautam, A. S., Srivastava, A. K., Kamra, A. K.,
499 Soni, V. K., and Sethi, V.: Observations of new particle formation at two distinct Indian
500 subcontinental urban locations, *Atmos. Environ.*, 96, 370-379, Doi:
501 10.1016/j.atmosenv.2014.08.001, 2014.

502 Köllner, F., Schneider, J., Willis, M. D., Klimach, T., Helleis, F., Bozem, H., Kunkel, D., Hoor,
503 P., Burkart, J., Leaitch, W. R., Aliabadi, A. A., Abbatt, J. P. D., Herber, A. B., and
504 Borrmann, S.: Particulate trimethylamine in the summertime Canadian high Arctic lower
505 troposphere, *Atmos. Chem. Phys.*, 17, 13747-13766, 10.5194/acp-17-13747-2017, 2017.

506 Kürten, A., Bergen, A., Heinritzi, M., Leiminger, M., Lorenz, V., Piel, F., Simon, M., Sitals, R.,
507 Wagner, A. C., and Curtius, J.: Observation of new particle formation and measurement
508 of sulfuric acid, ammonia, amines and highly oxidized organic molecules at a rural site in
509 central Germany, *Atmos. Chem. Phys.*, 16, 12793-12813, 10.5194/acp-16-12793-2016,
510 2016.

511 Lee, S.-H.: Perspective on the Recent Measurements of Reduced Nitrogen Compounds in the
512 Atmosphere, *Frontiers in Environmental Science*, 10, 10.3389/fenvs.2022.868534, 2022.

513 Lee, S.-H., Gordon, H., Yu, H., Lehtipalo, K., Haley, R., Li, Y., and Zhang, R.: New Particle
514 Formation in the Atmosphere: From Molecular Clusters to Global Climate, *Journal of
515 Geophysical Research: Atmospheres*, 124, 7098-7146, 10.1029/2018JD029356, 2019.

516 Leen, J. B., Yu, X.-Y., Gupta, M., Baer, D. S., Hubbe, J. M., Kluzek, C. D., Tomlinson, J. M.,
517 and Hubbell, M. R., II: Fast In Situ Airborne Measurement of Ammonia Using a Mid-
518 Infrared Off-Axis ICOS Spectrometer, *Environmental Science & Technology*, 47, 10446-
519 10453, 10.1021/es401134u, 2013.

520 Lehtipalo, K., Yan, C., Dada, L., Bianchi, F., Xiao, M., Wagner, R., Stolzenburg, D., Ahonen, L.
521 R., Amorim, A., Baccharini, A., Bauer, P. S., Baumgartner, B., Bergen, A., Bernhammer,
522 A.-K., Breitenlechner, M., Brilke, S., Buchholz, A., Mazon, S. B., Chen, D., Chen, X.,
523 Dias, A., Dommen, J., Draper, D. C., Duplissy, J., Ehn, M., Finkenzeller, H., Fischer, L.,
524 Frege, C., Fuchs, C., Garmash, O., Gordon, H., Hakala, J., He, X., Heikkinen, L.,
525 Heinritzi, M., Helm, J. C., Hofbauer, V., Hoyle, C. R., Jokinen, T., Kangasluoma, J.,
526 Kerminen, V.-M., Kim, C., Kirkby, J., Kontkanen, J., Kürten, A., Lawler, M. J., Mai, H.,
527 Mathot, S., Mauldin, R. L., Molteni, U., Nichman, L., Nie, W., Nieminen, T., Ojdanic,
528 A., Onnela, A., Passananti, M., Petäjä, T., Piel, F., Pospisilova, V., Quéléver, L. L. J.,
529 Rissanen, M. P., Rose, C., Sarnela, N., Schallhart, S., Schuchmann, S., Sengupta, K.,
530 Simon, M., Sipilä, M., Tauber, C., Tomé, A., Tröstl, J., Väisänen, O., Vogel, A. L.,
531 Volkamer, R., Wagner, A. C., Wang, M., Weitz, L., Wimmer, D., Ye, P., Ylisirniö, A.,
532 Zha, Q., Carslaw, K. S., Curtius, J., Donahue, N. M., Flagan, R. C., Hansel, A., Riipinen,
533 I., Virtanen, A., Winkler, P. M., Baltensperger, U., Kulmala, M., and Worsnop, D. R.:
534 Multicomponent new particle formation from sulfuric acid, ammonia, and biogenic
535 vapors, *Science Advances*, 4, eaau5363, 10.1126/sciadv.aau5363, 2018.

536 Liu, R., Liu, T., Huang, X., Ren, C., Wang, L., Niu, G., Yu, C., Zhang, Y., Wang, J., Qi, X., Nie,
537 W., Chi, X., and Ding, A.: Characteristics and sources of atmospheric ammonia at the

538 SORPES station in the western Yangtze river delta of China, *Atmospheric Environment*,
539 318, 120234, <https://doi.org/10.1016/j.atmosenv.2023.120234>, 2024.

540 Malloy, Q. G. J., Li, Q., Warren, B., Cocker Iii, D. R., Erupe, M. E., and Silva, P. J.: Secondary
541 organic aerosol formation from primary aliphatic amines with NO₃ radical,
542 *Atmos. Chem. Phys.*, 9, 2051-2060, 10.5194/acp-9-2051-2009, 2009.

543 Mao, J., Yu, F., Zhang, Y., An, J., Wang, L., Zheng, J., Yao, L., Luo, G., Ma, W., Yu, Q.,
544 Huang, C., Li, L., and Chen, L.: High-resolution modeling of gaseous methylamines over
545 a polluted region in China: source-dependent emissions and implications of spatial
546 variations, *Atmos. Chem. Phys.*, 18, 7933-7950, 10.5194/acp-18-7933-2018, 2018.

547 Martin, N. A., Ferracci, V., Cassidy, N., and Hoffnagle, J. A.: The application of a cavity ring-
548 down spectrometer to measurements of ambient ammonia using traceable primary
549 standard gas mixtures, *Applied Physics B*, 122, 219, 10.1007/s00340-016-6486-9, 2016.

550 McManus, J. B., Mark, S. Z., David, D. N., Jr., Joanne, H. S., Scott, C. H., Ezra, C. W., and
551 Rick, W.: Application of quantum cascade lasers to high-precision atmospheric trace gas
552 measurements, *Optical Engineering*, 49, 111124, 10.1117/1.3498782, 2010.

553 Miller, D. J., Sun, K., Tao, L., Khan, M. A., and Zondlo, M. A.: Open-path, quantum cascade-
554 laser-based sensor for high-resolution atmospheric ammonia measurements, *Atmos.*
555 *Meas. Tech.*, 7, 81-93, 10.5194/amt-7-81-2014, 2014.

556 Myllys, N., Chee, S., Olenius, T., Lawler, M., and Smith, J.: Molecular-Level Understanding of
557 Synergistic Effects in Sulfuric Acid–Amine–Ammonia Mixed Clusters, *The Journal of*
558 *Physical Chemistry A*, 123, 2420-2425, 10.1021/acs.jpca.9b00909, 2019.

559 Nielsen, C. J.: Atmospheric Degradation of Amines (ADA). Summary report: Photo-oxidation of
560 methylamine, dimethylamine and trimethylamine. CLIMIT project no. 201604., Norge:
561 Norsk Institutt for Luftforskning, 2016.

562 Nielsen, C. J., Herrmann, H., and Weller, C.: Atmospheric chemistry and environmental impact
563 of the use of amines in carbon capture and storage (CCS), *Chemical Society Reviews*, 41,
564 6684-6704, 10.1039/C2CS35059A, 2012.

565 Nowak, J. B., Neuman, J. A., Bahreini, R., Brock, C. A., Middlebrook, A. M., Wollny, A. G.,
566 Holloway, J. S., Peischl, J., Ryerson, T. B., and Fehsenfeld, F. C.: Airborne observations
567 of ammonia and ammonium nitrate formation over Houston, Texas, *Journal of*
568 *Geophysical Research: Atmospheres*, 115, <https://doi.org/10.1029/2010JD014195>, 2010.

569 Nowak, J. B., Huey, L. G., Russell, A. G., Tian, D., Neuman, J. A., Orsini, D., Sjostedt, S. J.,
570 Sullivan, A. P., Tanner, D. J., Weber, R. J., Nenes, A., Edgerton, E., and Fehsenfeld, F.
571 C.: Analysis of urban gas phase ammonia measurements from the 2002 Atlanta Aerosol
572 Nucleation and Real-Time Characterization Experiment (ANARChE), *Journal of*
573 *Geophysical Research: Atmospheres*, 111, <https://doi.org/10.1029/2006JD007113>, 2006.

574 Petrus, M., Popa, C., and Bratu, A. M.: Ammonia Concentration in Ambient Air in a Peri-Urban
575 Area Using a Laser Photoacoustic Spectroscopy Detector, *Materials (Basel)*, 15,
576 10.3390/ma15093182, 2022.

577 Pollack, I. B., Lindaas, J., Roscioli, J. R., Agnese, M., Permar, W., Hu, L., and Fischer, E. V.:
578 Evaluation of ambient ammonia measurements from a research aircraft using a closed-
579 path QC-TILDAS operated with active continuous passivation, *Atmos. Meas. Tech.*, 12,
580 3717-3742, 10.5194/amt-12-3717-2019, 2019.

581 Pushkarsky, M. B., Webber, M. E., Baghdassarian, O., Narasimhan, L. R., and Patel, C. K. N.:
582 Laser-based photoacoustic ammonia sensors for industrial applications, *Applied Physics*
583 *B*, 75, 391-396, 10.1007/s00340-002-0967-8, 2002.

584 Qiu, C. and Zhang, R.: Multiphase chemistry of atmospheric amines, *Physical Chemistry*
585 *Chemical Physics*, 15, 5738-5752, 10.1039/C3CP43446J, 2013.

586 Schwab, J. J., Li, Y., Bae, M. S., Demerjian, K. L., Hou, J., Zhou, X., Jensen, B., and Pryor, S.
587 C.: A laboratory intercomparison of real-time gaseous ammonia measurement methods,
588 *Environ Sci Technol*, 41, 8412-8419, 10.1021/es070354r, 2007.

589 Silva, P. J., Erupe, M. E., Price, D., Elias, J., G. J. Malloy, Q., Li, Q., Warren, B., and Cocker, D.
590 R., III: Trimethylamine as Precursor to Secondary Organic Aerosol Formation via Nitrate
591 Radical Reaction in the Atmosphere, *Environmental Science & Technology*, 42, 4689-
592 4696, 10.1021/es703016v, 2008.

593 Smith, J. N., Barsanti, K. C., Friedli, H. R., Ehn, M., Kulmala, M., Collins, D. R., Scheckman, J.
594 H., Williams, B. J., and McMurry, P. H.: Observations of aminium salts in atmospheric
595 nanoparticles and possible climatic implications, *Proc. Natl. Acad. Sci.*, 107, 6634-6639,
596 2010.

597 Wang, G., Zhang, R., Gomez, M. E., Yang, L., Levy Zamora, M., Hu, M., Lin, Y., Peng, J., Guo,
598 S., Meng, J., Li, J., Cheng, C., Hu, T., Ren, Y., Wang, Y., Gao, J., Cao, J., An, Z., Zhou,
599 W., Li, G., Wang, J., Tian, P., Marrero-Ortiz, W., Secrest, J., Du, Z., Zheng, J., Shang,
600 D., Zeng, L., Shao, M., Wang, W., Huang, Y., Wang, Y., Zhu, Y., Li, Y., Hu, J., Pan, B.,
601 Cai, L., Cheng, Y., Ji, Y., Zhang, F., Rosenfeld, D., Liss, P. S., Duce, R. A., Kolb, C. E.,
602 and Molina, M. J.: Persistent sulfate formation from London Fog to Chinese haze,
603 *Proceedings of the National Academy of Sciences*, 113, 13630-13635,
604 10.1073/pnas.1616540113, 2016.

605 Wang, M., Kong, W., Marten, R., He, X.-C., Chen, D., Pfeifer, J., Heitto, A., Kontkanen, J.,
606 Dada, L., Kürten, A., Yli-Juuti, T., Manninen, H. E., Amanatidis, S., Amorim, A.,
607 Baalbaki, R., Baccarini, A., Bell, D. M., Bertozzi, B., Bräkling, S., Brilke, S., Murillo, L.
608 C., Chiu, R., Chu, B., De Menezes, L.-P., Duplissy, J., Finkenzeller, H., Carracedo, L. G.,
609 Granzin, M., Guida, R., Hansel, A., Hofbauer, V., Krechmer, J., Lehtipalo, K.,
610 Lamkaddam, H., Lampimäki, M., Lee, C. P., Makhmutov, V., Marie, G., Mathot, S.,
611 Mauldin, R. L., Mentler, B., Müller, T., Onnela, A., Partoll, E., Petäjä, T., Philippov, M.,
612 Pospisilova, V., Ranjithkumar, A., Rissanen, M., Rörup, B., Scholz, W., Shen, J., Simon,
613 M., Sipilä, M., Steiner, G., Stolzenburg, D., Tham, Y. J., Tomé, A., Wagner, A. C.,
614 Wang, D. S., Wang, Y., Weber, S. K., Winkler, P. M., Wlasits, P. J., Wu, Y., Xiao, M.,
615 Ye, Q., Zauner-Wieczorek, M., Zhou, X., Volkamer, R., Riipinen, I., Dommen, J.,
616 Curtius, J., Baltensperger, U., Kulmala, M., Worsnop, D. R., Kirkby, J., Seinfeld, J. H.,
617 El-Haddad, I., Flagan, R. C., and Donahue, N. M.: Rapid growth of new atmospheric
618 particles by nitric acid and ammonia condensation, *Nature*, 581, 184-189,
619 10.1038/s41586-020-2270-4, 2020a.

620 Wang, Y., Yang, G., Lu, Y., Liu, Y., Chen, J., and Wang, L.: Detection of gaseous
621 dimethylamine using vocus proton-transfer-reaction time-of-flight mass spectrometry,
622 *Atmospheric Environment*, 243, 117875,
623 <https://doi.org/10.1016/j.atmosenv.2020.117875>, 2020b.

624 Xiao, M., Hoyle, C. R., Dada, L., Stolzenburg, D., Kürten, A., Wang, M., Lamkaddam, H.,
625 Garmash, O., Mentler, B., Molteni, U., Baccarini, A., Simon, M., He, X. C., Lehtipalo,
626 K., Ahonen, L. R., Baalbaki, R., Bauer, P. S., Beck, L., Bell, D., Bianchi, F., Brilke, S.,
627 Chen, D., Chiu, R., Dias, A., Duplissy, J., Finkenzeller, H., Gordon, H., Hofbauer, V.,
628 Kim, C., Koenig, T. K., Lampilahti, J., Lee, C. P., Li, Z., Mai, H., Makhmutov, V.,
629 Manninen, H. E., Marten, R., Mathot, S., Mauldin, R. L., Nie, W., Onnela, A., Partoll, E.,

630 Petäjä, T., Pfeifer, J., Pospisilova, V., Quéléver, L. L. J., Rissanen, M., Schobesberger, S.,
631 Schuchmann, S., Stozhkov, Y., Tauber, C., Tham, Y. J., Tomé, A., Vazquez-Pufleau, M.,
632 Wagner, A. C., Wagner, R., Wang, Y., Weitz, L., Wimmer, D., Wu, Y., Yan, C., Ye, P.,
633 Ye, Q., Zha, Q., Zhou, X., Amorim, A., Carslaw, K., Curtius, J., Hansel, A., Volkamer,
634 R., Winkler, P. M., Flagan, R. C., Kulmala, M., Worsnop, D. R., Kirkby, J., Donahue, N.
635 M., Baltensperger, U., El Haddad, I., and Dommen, J.: The driving factors of new particle
636 formation and growth in the polluted boundary layer, *Atmos. Chem. Phys.*, 21, 14275-
637 14291, 10.5194/acp-21-14275-2021, 2021.

638 Xiao, S., Wang, M. Y., Yao, L., Kulmala, M., Zhou, B., Yang, X., Chen, J. M., Wang, D. F., Fu,
639 Q. Y., Worsnop, D. R., and Wang, L.: Strong atmospheric new particle formation in
640 winter in urban Shanghai, China, *Atmos. Chem. Phys.*, 15, 1769-1781, 10.5194/acp-15-
641 1769-2015, 2015.

642 Yan, C., Yin, R., Lu, Y., Dada, L., Yang, D., Fu, Y., Kontkanen, J., Deng, C., Garmash, O.,
643 Ruan, J., Baalbaki, R., Schervish, M., Cai, R., Bloss, M., Chan, T., Chen, T., Chen, Q.,
644 Chen, X., Chen, Y., Chu, B., Dällenbach, K., Foreback, B., He, X., Heikkinen, L.,
645 Jokinen, T., Junninen, H., Kangasluoma, J., Kokkonen, T., Kurppa, M., Lehtipalo, K., Li,
646 H., Li, H., Li, X., Liu, Y., Ma, Q., Paasonen, P., Rantala, P., Pileci, R. E., Rusanen, A.,
647 Sarnela, N., Simonen, P., Wang, S., Wang, W., Wang, Y., Xue, M., Yang, G., Yao, L.,
648 Zhou, Y., Kujansuu, J., Petäjä, T., Nie, W., Ma, Y., Ge, M., He, H., Donahue, N. M.,
649 Worsnop, D. R., Veli-Matti, K., Wang, L., Liu, Y., Zheng, J., Kulmala, M., Jiang, J., and
650 Bianchi, F.: The Synergistic Role of Sulfuric Acid, Bases, and Oxidized Organics
651 Governing New-Particle Formation in Beijing, *Geophysical Research Letters*, 48,
652 e2020GL091944, <https://doi.org/10.1029/2020GL091944>, 2021.

653 Yao, L., Wang, M. Y., Wang, X. K., Liu, Y. J., Chen, H. F., Zheng, J., Nie, W., Ding, A. J.,
654 Geng, F. H., Wang, D. F., Chen, J. M., Worsnop, D. R., and Wang, L.: Detection of
655 atmospheric gaseous amines and amides by a high-resolution time-of-flight chemical
656 ionization mass spectrometer with protonated ethanol reagent ions, *Atmos. Chem. Phys.*,
657 16, 14527-14543, 10.5194/acp-16-14527-2016, 2016.

658 You, Y., Kanawade, V. P., de Gouw, J. A., Guenther, A. B., Madronich, S., Sierra-Hernández,
659 M. R., Lawler, M., Smith, J. N., Takahama, S., Ruggeri, G., Koss, A., Olson, K.,
660 Baumann, K., Weber, R. J., Nenes, A., Guo, H., Edgerton, E. S., Porcelli, L., Brune, W.
661 H., Goldstein, A. H., and Lee, S. H.: Atmospheric amines and ammonia measured with a
662 Chemical Ionization Mass Spectrometer (CIMS), *Atmos. Chem. Phys.*, 14, 12181-
663 12194, Doi: 10.5194/acpd-14-16411-2014, 2014.

664 Yu, H. and Lee, S. H.: A chemical ionization mass spectrometer for the detection of atmospheric
665 amines, *Environ. Chem.*, 9, 190-201, 2012

666 Yu, H., McGraw, R., and Lee, S. H.: Effects of amines on formation of sub-3 nm particles and
667 their subsequent growth, *Geophys. Res. Lett.*, 39, Doi: 10.1029/2011gl050099,
668 10.1029/2011gl050099, 2012.

669 Zhao, B., Donahue, N. M., Zhang, K., Mao, L., Shrivastava, M., Ma, P.-L., Shen, J., Wang, S.,
670 Sun, J., Gordon, H., Tang, S., Fast, J., Wang, M., Gao, Y., Yan, C., Singh, B., Li, Z.,
671 Huang, L., Lou, S., Lin, G., Wang, H., Jiang, J., Ding, A., Nie, W., Qi, X., Chi, X., and
672 Wang, L.: Global variability in atmospheric new particle formation mechanisms, *Nature*,
673 631, 98-105, 10.1038/s41586-024-07547-1, 2024.

674 Zheng, J., Ma, Y., Chen, M., Zhang, Q., Wang, L., Khalizov, A. F., Yao, L., Wang, Z., Wang,
675 X., and Chen, L.: Measurement of atmospheric amines and ammonia using the high

676 resolution time-of-flight chemical ionization mass spectrometry, Atmospheric
677 Environment, 102, 249-259, <https://doi.org/10.1016/j.atmosenv.2014.12.002>, 2015.
678 Zhu, S., Yan, C., Zheng, J., Chen, C., Ning, H., Yang, D., Wang, M., Ma, Y., Zhan, J., Hua, C.,
679 Yin, R., Li, Y., Liu, Y., Jiang, J., Yao, L., Wang, L., Kulmala, M., and Worsnop, D. R.:
680 Observation and Source Apportionment of Atmospheric Alkaline Gases in Urban
681 Beijing, Environmental Science & Technology, 56, 17545-17555,
682 10.1021/acs.est.2c03584, 2022.
683